

Article

Shape Analysis of Prosthetic Socket Rectification Procedure for Transtibial Amputees

Yogeshvaran R. Nagarajan ¹, Farukh Farukh ^{1,2,*} , Vadim V. Silberschmidt ³ , Karthikeyan Kandan ¹, Amit Kumar Singh ^{4,5} and Pooja Mukul ⁶

¹ Institute of Engineering Sciences, School of Engineering and Sustainable Development, De Montfort University, The Gateway, Leicester LE1 9BH, UK

² Faculty of Engineering, Universitas Negeri Padang, Padang 25131, Indonesia

³ Wolfson School of Mechanical, Electrical and Manufacturing Engineering, Loughborough University, Loughborough LE11 3TU, UK

⁴ Department of Mechanical Engineering, Malaviya National Institute of Technology, Jaipur 302017, India

⁵ Department of Mechanical Engineering, National Institute of Technology Calicut, Calicut 673601, India

⁶ Bhagwan Mahaveer Viklang Sahayata Samiti (BMVSS), Jaipur 302017, India

* Correspondence: f.farukh@dmu.ac.uk

Abstract: Achieving a comfortable socket residual limb interface is crucial for effective prosthetic rehabilitation, depending on the precise characterisation and fluctuations in the shape and volume of residual limbs. Clinicians rely on subjective and iterative methods for shaping sockets, often involving a trial-and-error approach. This study introduces a framework for measuring, analysing, and comparing residual limb shape and volume using scanned data to facilitate more informed clinical decision-making. Surface scans of 44 transtibial residual limb casts of various sizes and lengths were examined. All scans were spatially aligned to a mid-patella and subjected to analysis using a shape analysis toolbox. Geometric measurements were extracted, with particular attention to significant rectified regions during the cast rectification process. Following PTB guidelines, our analysis revealed substantial alterations, primarily in the mid-patella region, followed by the patellar tendon area. Notably, there was a significant volume change of 6.02% in the region spanning from mid-patella to 25% of the cast length. Beyond this point, linear cast modifications were observed for most amputees up to 60% of the cast length, followed by individual-specific deviations beyond this region. Regardless of residual limb size and length, the modifications applied to positive casts suggested categorising patients into five major groups. This study employs the AmpScan shape analysis tool, to comprehend the cast rectification process used for capturing and assessing the extent of rectification on patients' residual limb casts. The clinical implications of our research are threefold: (a) the comparison data can serve as training resources for junior prosthetists; (b) this will aid prosthetists in identifying specific regions for rectification and assessing socket fit; (c) it will help in determining optimal timing for prosthetic fitting or replacement.

Keywords: transtibial amputees; prosthetic socket; 3D scanning; AmpScan; cast rectification procedure



Citation: Nagarajan, Y.R.; Farukh, F.; Silberschmidt, V.V.; Kandan, K.; Singh, A.K.; Mukul, P. Shape Analysis of Prosthetic Socket Rectification Procedure for Transtibial Amputees. *Prosthesis* **2024**, *6*, 157–174. <https://doi.org/10.3390/prosthesis6010013>

Academic Editor: Giuseppina Gini

Received: 8 December 2023

Revised: 25 January 2024

Accepted: 29 January 2024

Published: 5 February 2024



Copyright: © 2024 by the authors. Licensee MDPI, Basel, Switzerland. This article is an open access article distributed under the terms and conditions of the Creative Commons Attribution (CC BY) license (<https://creativecommons.org/licenses/by/4.0/>).

1. Introduction

A prosthesis is an external device used to replace missing or impaired body parts. Technological advancements in prosthetics have the potential to directly enhance the functional capabilities and mobility of patients with limb amputations. For lower limb amputees, a prosthesis typically comprises three essential components: a socket, a pylon, and a foot. Among these components, the socket is a crucial link connecting the residual limb to the remainder of the prosthesis. Furthermore, it is critical for effective load transfer during the gait cycle. Inadequate socket design can lead to discomfort in walking, residuum pain, skin related problems, alternated gait biomechanics, and so on [1–3]. Thus, ensuring

an appropriate interface between the residual limb and the prosthetic socket is paramount, as it directly influences an amputee's ability to perform daily activities.

Traditionally, prosthetic sockets are manufactured using high-density polyethylene, polypropylene, and other monolithic thermoplastic materials. Alternatively, high-performance fibre-reinforced composite lamination techniques are also employed for socket manufacturing [4]. Regardless of the method chosen, the process relies heavily on the shape of the limb cast, which is developed with various casting techniques. However, it is worth noting that computer-aided design and manufacturing (CAD/CAM) methods have emerged as an alternative approach to socket creation, although these are less popular, especially in low–middle-income countries (LMICs).

One widely adopted casting method for socket manufacturing is the patellar tendon bearing (PTB) method, designed to distribute the primary body weight onto the patellar tendon region [5,6]. However, PTB cast modification involves labour-intensive processes, with clinicians identifying tolerant and intolerant regions on the residual limb. Besides this, there are a relatively limited number of experts in cast rectification compared to the number of global amputees [7]. However, such manual adjustments are time-consuming and often lack consistency in achieving an optimal socket fit [8,9]. For instance, P. Convery et al. showed the inconsistency in the rectification of the cast between two prosthetists [10]. Presently, the design of a comfortable prosthetic socket is not only manual but an art mainly dependent on a prosthetist's skill and experience [11]. The total surface bearing (TSB) method was developed to address the limitations associated with weight-bearing PTB methods, aiming to achieve uniform pressure distribution across the stump's surface [12]. Despite its potential benefits, TSB cast modification can be challenging for residual limbs, with significant volume changes. To overcome this, the concept of pressure casting, also known as hydrostatic or hydrocast, was introduced [13]. This innovative approach uses fluid as a loading medium to ensure uniform pressure across the residual limb, adhering to Pascal's law of fluids. However, hydrocasts may not be suitable for amputees with prominent distal tibia and loose soft tissue, and their practical utility is yet to be established in real-life scenarios [14–16].

Recognising the need for consistent residuum casts, the CAD/CAM technology emerged as a solution for capturing residual limb shapes and rectifying them using 3D modelling software. Integrating digital technology into prosthetics significantly enhanced both their function and aesthetics while reducing the required time compared to traditional methods [17,18]. With the increasing availability of surface scanning technology, digital tools were developed to assess cast rectification and shape deviation. Indeed, automated shape analysis software allows clinicians to evaluate 3D scans of residual limbs and monitor clinical progress.

Prominent among these tools is ShapeMaker, a socket rectification software developed as part of the VA's Automated Fabrication of Mobility Aids (AFMA) initiative. Additionally, Colombo and Buzzi [19,20] developed an advanced socket modelling assistant capable of importing clinical parameters to aid cast rectification. However, these advanced modelling techniques often require limb models generated with expensive imaging devices like MRI or CT scanners. WillowWood's Omega stands out as another widely adopted commercial package in the prosthetic field [21]. The software allows clinicians to import residual limb models that are either measured or scanned, and then align and rectify the model according to the preferred workflow. Similarly, NiaFit is another socket rectification software built on Autodesk Meshmixer that facilitates the Virtual Reality (VR) environment with a streamlined workflow for socket rectification [22]. In this regard, studies were undertaken using a machine learning (ML) algorithm to examine the datasets of the socket design [23–25]. For instance, socket–limb interface pressures were predicted using artificial neural networks (ANN) based on non-invasive socket strain measurements. Similarly, Karamousadakis et al. employed the fuzzy logic Inference Engine (IE) to develop a decision support system (DSS) to transform the pressure measurements into socket rectifications [26,27]. In response to the growing accessibility of digital scanners, Steer [28] developed an open-source Python-

based shape analysis package. This software enables the comparison of pairs of surface scans through alignment, registration, and visualisation, allowing the extraction of crucial measurements to evaluate the consistency, accuracy, and reliability of casting techniques and surface scanners.

Clinicians traditionally rely on residual limb volume and circumferential measurements to determine socket replacement needs [16]. However, the residual limb affects the shape and volume, especially during the initial post-operative phase following amputation. Various methods have been proposed in the literature to measure the residual limb volume, including anthropometric measurements and water immersion techniques. While these methods are accurate, they are time-consuming, have limited repeatability, and may be affected by the movements and positions of patients. Advanced techniques, such as MRI, CT and ultrasound scans, offer greater accuracy but are costly, time-intensive, and less practical for clinical use [29,30].

Laser scanning technology, part of the CAD/CAM system, was introduced to overcome these limitations. Subsequently, this method projects planes of laser light onto the residual limb surface, recording the shape as it interacts with the limb. A three-dimensional model can be constructed from these data, allowing for accurate volume measurement. Laser scanning provides accurate shape and volume data for residual limbs, efficiently accommodates minor patient movements, and facilitates anatomical feature detection. Consequently, computer-aided volume and shape measurements with laser-based scanning technology were adopted to visualise the residual limb geometry and monitor changes over time, supporting the identification of high-pressure areas [31,32].

Despite the advantages of laser scanning, clinicians often continue to rely on subjective methods, including personal judgment and user feedback, in the socket design process [33]. In busy clinical settings, having access to detailed shape and volumetric measurement and comparison tools that are both affordable and user-friendly would be ideal. Currently, there is a lack of quantitative matrices for clinicians to monitor changes in residual limb geometry, assess the socket fit, or predict when socket replacement is necessary.

This study seeks to address these challenges by employing a high-accuracy 3D surface scanning and shape analysis toolbox to assess the correction procedures applied to sockets for managing residual limbs. By capturing critical features of the cast rectification process, the aim is to generate a comprehensive set of clinically relevant shape metrics at significant areas of residual limbs. This study provides insights into the trends in socket design by expert clinicians, leading to the proposal of a socket design template. Such a template can potentially reduce the workload of expert clinicians during the socket design process while supporting junior clinicians in understanding the intricacies of socket design. This tool is particularly valuable for LMIC, where the demand for prostheses often exceeds the availability of expert clinicians.

In summary, this research combines high-precision 3D scanning and shape analysis to comprehensively evaluate the socket correction procedures for residual limbs, contributing to advancing evidence-based socket design processes. While this approach does not seek to eliminate the need for clinical expertise, it aims to streamline the design of definitive sockets, reducing the time-consuming trial-and-error iterations typically associated with socket design.

2. Materials and Methods

The De Montfort University Ethical Review Committee approved this study (Research Ethics Application Approval: 1920/553), and the required informed consent was obtained from the subjects before participation.

2.1. Participants

A diverse set of forty-four transtibial residual limb models were used for this investigation. Both unrectified casts (URC) and rectified casts (RC) were 3D-scanned for all forty-four residual limbs. Prior to their use in this study, all cast data were de-identified.

Participants were conveniently recruited from a single prosthetic facility in India. Table 1 provides essential statistical details about the participants.

Table 1. Descriptive statistics of amputees that participated in the study.

Parameters	Values
Age (mean) (median) (standard deviation)	44.6 (46) (16.92)
Gender	
Male	38
Female	6
Unilateral	37
Bilateral	7
Years since amputation (mean) (median) (standard deviation)	10.24 (6) (8.20)
Causes of amputation	
Trauma	31
Vascular	13
Occupation	
Unemployed	10
Office worker	2
Driver	2
Homemaker	5
Student	7
Business	13
Farmer	5

2.2. Manufacturing Process

BMVSS employs the PTB cast technique for socket manufacturing. This casting process starts with biomechanical markings made on a cling film-wrapped residual limb (step I in Figure 1). Subsequently, a negative cast of the limb is created using plaster of Paris (PoP) bandage, resulting in the production of a positive cast, also known as the unmodified or unrectified cast (URC), which serves as the foundation for socket fabrication (step II and III in Figure 1).

The cast is then subjected to a modification based on pressure-sensitive and pressure-tolerant areas around the limb, resulting in what is referred to as a modified or rectified cast (RC) (step IV in Figure 1). Typically, material is removed from the regions where additional load-bearing capacity is feasible. In contrast, material is added to the sensitive areas. Once the cast is rectified, a pre-heated HDPE sleeve is draped over it to craft the final socket. Figure 1a illustrates the traditional manufacturing process of the monolithic thermoplastic socket. Such casts are expertly fabricated by prosthetists and clinicians at BMVSS, representing the standard positive mold employed in socket production at their facility.

2.3. Data Collection

Via the above-discussed process, we proceed after the positive URC stage to the 3D-scanning of the cast. Subsequently, prosthetists rectified the cast based on PTB principles, and then, the RC were also 3D-scanned. For scanning the RC and URC, an EinScan Pro 3D (Shining 3D Tech. Co., Ltd., Hangzhou, China) laser scanner was used by an expert assessor. The EinScan 3D scanner has a resolution of 0.04 mm in a Fixed Scan Mode. When operating in a handheld scanning mode with marker alignment, it achieves volumetric accuracy, reaching up to 0.045 mm + 0.3 mm/m. It has been rigorously tested and calibrated for its accuracy according to VDI/VDE 2634 standards.



Figure 1. The workflow for evaluating the correction procedure in this study: (a) typical socket manufacturing process followed by BMVSS; (b) three-dimensional laser-scanned unmodified and modified casts; (c) stages of the shape analyses toolbox from misaligned surface scans to pairwise cast quantification.

Conversely, the positive casts were stabilised on the table to capture their surface shape. The setup and scan time for each patient was around 30 min. In consideration of the significant impact of material and colour on scan quality, spherical adhesive markers with a 4 mm diameter were strategically placed in accordance with the manufacturer's guidelines to enhance scan accuracy. Additionally, while we did not use a precision-enhancing spray, we meticulously followed the recommended practices for marker placement to optimize the scanning process. This approach aimed at mitigating potential challenges associated with material and colour variations, ensuring a more accurate and reliable scan outcome. There were two phases of the measurements: (a) the scanning of the casts and (b) the post-processing and regeneration of the cast in a computer. For the scanning phase, the assessor marked the models to designate the volume of interest. Markings were made to provide a point of reference for the scanner to capture the required data. Following that, the casts were scanned, and thus, the patient's metadata were revealed for the study.

Furthermore, the scanning phase was followed by the post-processing stage, with the assessor extracting the shape and volumetric measurements independently in the computer environment. To examine the 3D models, the scanned cast was exported in the stereolithography (.stl) format for shape analysis. The 3D-scanned URC and RC are shown in Figure 1b. However, to recreate the cast in CAD, a plane was established using the distal borders of these markers, serving as the reference for the proximal end of each scan.

2.4. Calibration Test and Validity of Data

The data's accuracy is critical in a clinical environment, and is directly linked to the comfort and life of the prosthetic socket. Due to the nature of the laser scanning process and its phases (as mentioned in the previous section), shape errors may appear in the data, leading to an inaccurate fit of the final socket.

To assess the validity and reliability of the scanner, calibration tests were performed using a CAD model with a combination of flat, convex and concave surfaces. Because of the complex shape of the limb and the use of PoP for casting, a negative model of the below CAD model was additively manufactured. Following that, PoP was used to get the positive cast, and thus, the shape error was analysed by comparing it with the parent CAD model. Apart from the validation of the scanner, the primary focus was to examine the scanner on PoP, as measurements can be affected by the characteristics of surface reflectivity and texture. The 3D model and the cross-section plot are illustrated in Figure 2. Their comparison using the shape analysis toolbox (briefly explained in Section 2.5) resulted in minor errors of 1.48%, 1.19% and 1.81% for the flat, concave and convex surfaces, respectively. The scanner calibration process was identical to the socket scan, i.e., based on two phases: (a) scanning of the casts and (b) post-processing. The validity of the scanner is determined by the extent of similarity between the measurements and the actual volume of the object. The data were collected several times and measured for variations to estimate the scanner's reliability. It is worth mentioning here that the study involved the intra-rater reliability of the scanner.

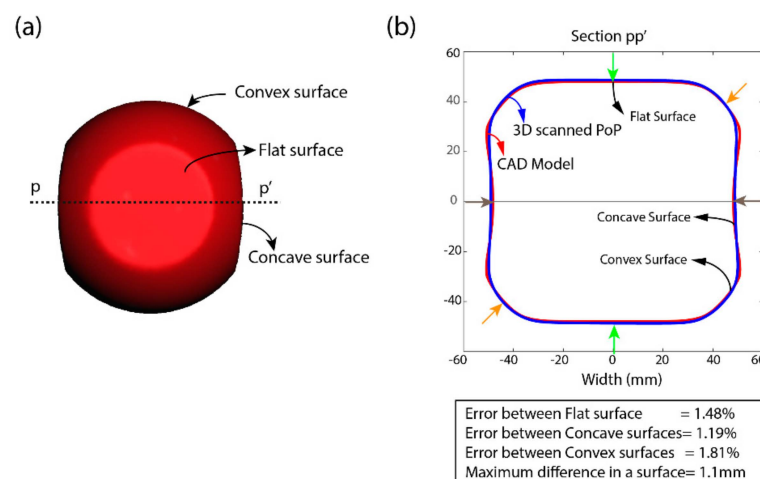


Figure 2. The measured calibrated model of the 3D scanner using shape analysis toolbox; (a) CAD model with flat, convex and concave shape; (b) cross-sectional slice of CAD model and 3D-scanned PoP cast with arrows (green-flat, orange-convex, black-concave) representing the limits of surface.

2.5. Shape Analysis

To assess the limb shape and socket design, the scan data were analysed with a Python-based open-source shape analysis toolbox Ampscan [28]. AmpScan 0.2 is a dedicated software package explicitly designed for 3D scanning analysis in the fields of prosthetics and orthotics. The package can be used either through a Graphical User Interface (GUI) or directly through Python functions. Though many types of shape analysis software exist, the Ampscan is tailored to have exceptional capabilities, is user-friendly, and is an open-source package, making it more advantageous for researchers and clinicians. The workflow of the software begins by importing and visualising the pair of scans into the python environment. The postprocessing steps in our study involved the alignment of the mid-patella in unrectified and rectified casts. Beyond this alignment, no further postprocessing was performed. Specifically, on the 3D scan data, no additional processing was applied, including within AmpScan. Although AmpScan employs a Laplacian approach for continuous cast smoothing, it was intentionally avoided in our analysis to prevent

potential feature and volume loss. Consequently, the scanned data were analysed without any smoothing of the surface to ensure accurate representation.

To standardise the process and enable data comparisons for several amputees at a time, all the casts were aligned by origin at the mid-patella region using Autodesk Meshmixer. A pair of datasets, with a surface mesh in the form of *.stl file formats, for each patient, i.e., scanned URC and corresponding RC, was brought into the Ampscan environment (step IX in Figure 1c). AmpScan aligned the data files using an Iterative Closest Point (ICP) algorithm. Following that, we assessed the shape deviation between the imported scans (steps X and XI). The scanned URC and RC data were aligned in the 3D space (i.e., the principle axis of the cast shape was in line with the global vertical axis in the sagittal plane) using an automated option provided by the algorithm. The workflow of AmpScan is illustrated in Figure 1c. Admittedly, the software provided overlapped and aligned shapes with the same number of vertices and level of connectivity as the baseline to enable direct shape and volume comparisons, with the red area of shape deviation indicating the modified regimes (pressure-sensitive areas) and the blue areas corresponding to unmodified regions (pressure-tolerant areas). Due to the complexity of the shape and data processing, the analysis section of the algorithm converts the 3D object into 2D shapes. The 3D objects were sliced into sequential cross-sections, which provide precise and comprehensive analysis results. Once the casts were aligned and processed for shape deviation, both casts of each amputee were finely sliced at 2 mm intervals along the cast length (CL) and analysed with respect to different parameters such as perimeter, cross-sectional area, volume, as well as the sagittal and coronal width of the casts.

The range of parameters was extracted for data analysis with the shape analysis toolbox. The conventional measurements of the residual limb and the rectified casts are the volume, perimeter and length. The analysis was performed using these parameters to establish general trends and co-relation in the correction procedure. Upon the 3D plotting of the volume, perimeter and length data, the amputees were permeated over a large area without any likeliness (Figure 3). The length of the residual limb ranged from 140 mm to 320 mm for the scanned participants. To achieve a comparison over these ranges, the cast length was normalised in percentage by aligning 0 at the mid-patella.

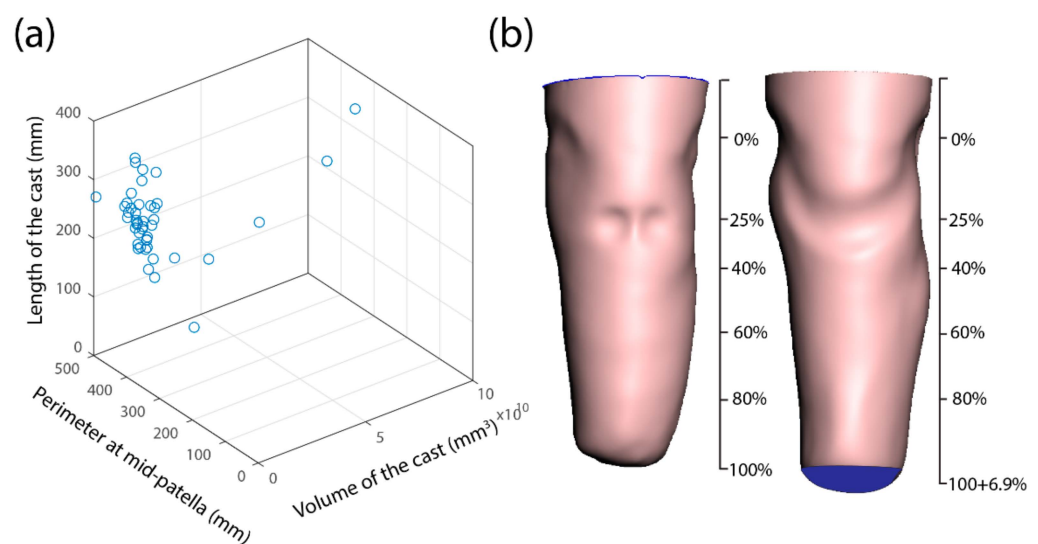


Figure 3. Comparison of the three-dimensional plot of volume, perimeter and length of unrectified cast (a); percentage length of the unrectified and rectified cast (b).

To quantify the rectification process undertaken by the prosthetist, the AmpScan data were extracted as a *.mat file and examined using MATLAB (MathWorks, Natick, MA, USA). The data were analysed to derive an insight into the expert clinicians' socket design and

establish the general trends in the socket design process to propose a socket design space for junior clinicians. Figure 3b represents the aligned URC and RC of the single subject.

3. Results

To gain a comprehensive grasp of the cast's dimensional characteristics, both RC and URCs were analysed in terms of their perimeter, sagittal width, and coronal width. Table 2 represents the absolute mean difference and standard deviation of these parameters. Furthermore, Figure 4a demonstrates a single patient's perimeter, as well as its sagittal and coronal responses along its normalised length. On the other hand, Figure 4b–d illustrate the mean differences between RC and URC of all subjects with respect to the abovementioned parameters. Our examination primarily focused on the region extending from the mid-patella to the distal stump end. The significant findings emerged in the perimeter, with the most substantial difference observed at MP, followed by a linear decline until the 25% cast length; this area is particularly noteworthy due to the presence of the patellar tendon. Subsequently, the mean value exhibited a steady progression until the 60% cast length, after which differences started to deviate, showing considerable variations among different subjects.

Table 2. The measured difference between rectified and unrectified casts along its length.

Percentage Length of Cast (%)	Diff in Perimeter Mean (SD) (mm)	Diff in Coronal Width Mean (SD) (mm)	Diff in Sagittal Width Mean (SD) (mm)
0 (Mid Patella)	18.00 (10.45)	−0.25 (3.25)	6.05 (5.00)
10	8.66 (14.42)	−0.74 (3.00)	0.36 (7.50)
25	−4.48 (9.00)	−0.18 (2.65)	−4.56 (5.49)
40	−0.27 (10.61)	−0.82 (4.21)	2.01 (4.58)
50	1.25 (10.47)	−0.79 (4.18)	3.36 (4.64)
60	1.75 (10.22)	−1.08 (3.96)	3.58 (4.68)
70	2.32 (10.26)	−1.73 (3.62)	4.60 (4.85)
80	8.40 (13.41)	−0.81 (4.34)	7.02 (6.06)
90	27.33 (22.02)	3.86 (6.32)	14.16 (9.55)
100	49.43 (50.90)	12.08 (15.63)	19.20 (18.55)

The mean sagittal width exhibited a similar trend, highlighting that most of the modification occurred on the sagittal side of the socket. However, a linear increase in mean difference was observed beyond the patellar tendon region. In contrast, the coronal width in Figure 4c established a steady mean value until the distal end of the stump. However, the increase in the distal region depended on the nature of the distal end of the stump.

In summary, our analysis has revealed significant rectification at MP as well as 10% and 25% of the cast length, with uniform rectification at the mid-stump. The deviation in the perimeter beyond 60% was inconsistent, leading to the division of the validation of this study into two categories for analysis:

- Analysis of significant regions up to the 60% mark of the cast length;
- Examination of the consistency in deviation beyond the 60% mark.

3.1. Evaluation of Cross-Sectional Area

Given the significant rectification observed at MP and as 10% and 25% of the cast length, it is crucial to analyse these regions so as to assess the correction process. Although previous studies considered the extent of rectification in specific tolerance-sensitive areas, they neglected the cross-sectional area. The reason is that the cast is typically modified around its circumference, rather than locally. Hence, the cross-sectional profiles of these significant areas were charted to validate the rectification across 360°.

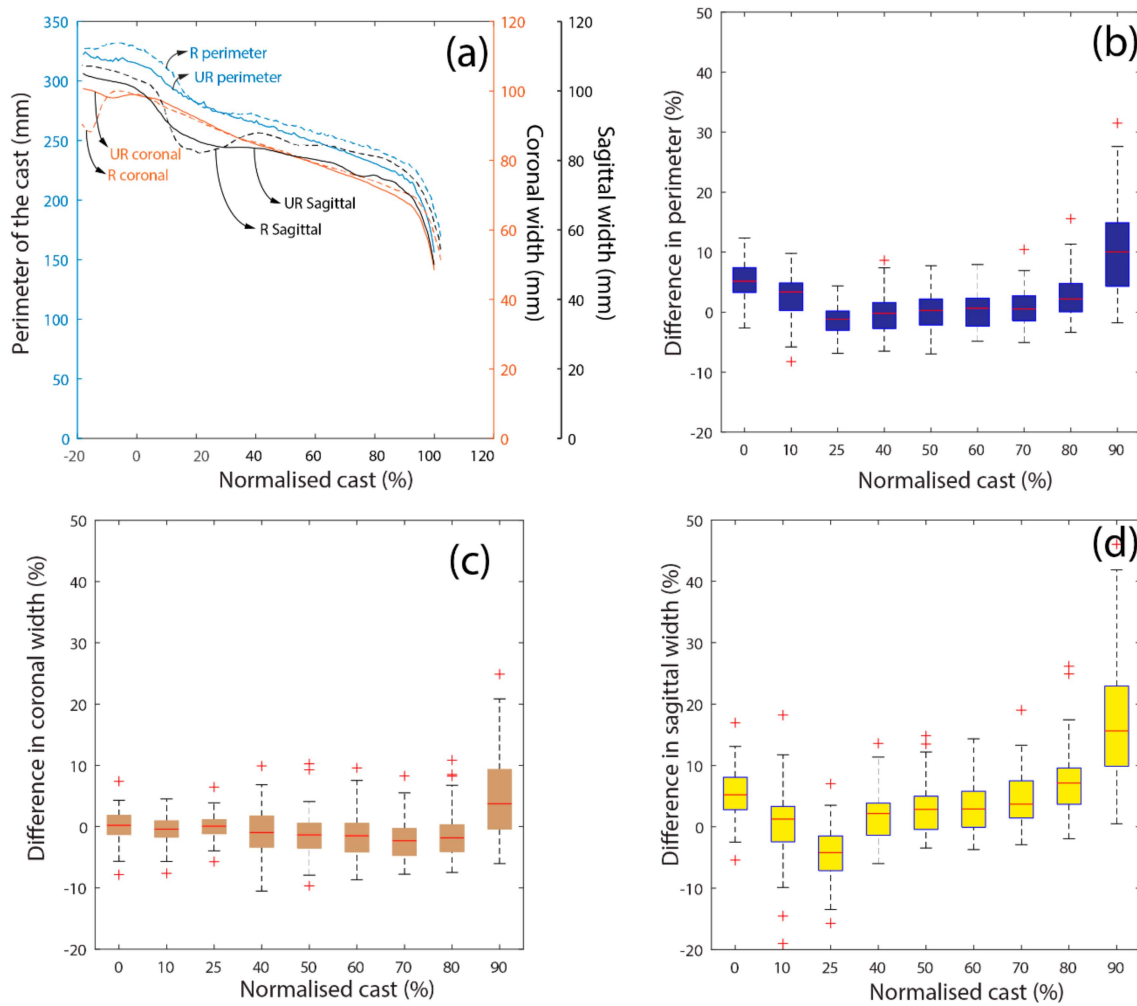


Figure 4. The measured perimeter, coronal and sagittal responses of an amputee (a); the difference between the rectified and unrectified casts along the normalised length for (b) perimeter (c) coronal width and (d) sagittal width. The + indicates the maximum and minimum absolute values.

Furthermore, the cast at the mid-stump (50%) was also assessed. In this regard, the extracted datasets of URC and RC were analysed at specific axial levels corresponding to MP, as well as 10%, 25% and 50% of the cast length. Figure 5 illustrates sample plots showcasing the aligned URC and RC and the cross-sectional area of four randomly selected subjects. The red region on the aligned cast represents the modified areas, while the blue region represents that which remained unaltered during rectification.

Notably, regardless of the stump’s length or shape, a consistent correction trend was evident for these subjects. For instance, at the mid-patella, an increase in posterior flare length and a reduction in posterior lateral and posterior medial dimensions were observed, together with a slight increase in the anterior cast. Similarly, at 25% of the cast length, the pressure distribution at the popliteal fossa (PF) (posterior curve) appeared comparable among amputees. In contrast, the mid-stump (50%) showed nearly uniform distribution around the circumference.

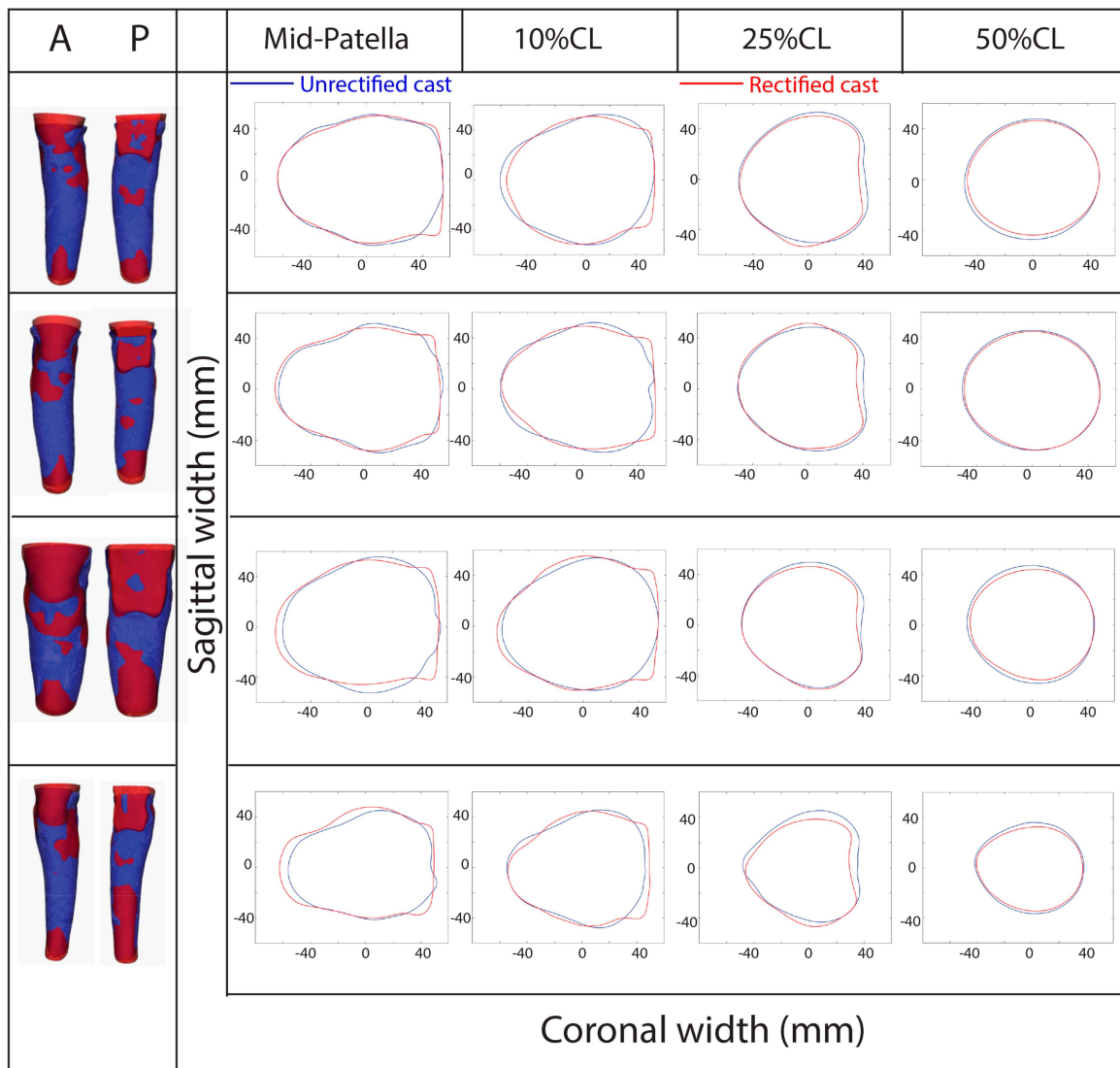


Figure 5. The samples of aligned casts and cross-sectional areas at mid-patella, 10%, 25% and 50% of cast length. A and P demonstrate the anterior and posterior of the aligned cast.

This comprehensive analysis demonstrates the importance of an in-depth circumferential assessment for all subjects. The slicing of the URC and the RC at MP, with 0 degrees set as the posterior cast, is shown in Figure 6a. Subsequently, the assessment was performed in an anti-clockwise manner by measuring the axial distance between RC and URC around the circumference. However, all validations were made with respect to the centroid of the URC as a reference point. The extent of rectification at MP, 10%, 25%, and 50% of the cast length is depicted in Figure 6.

Although deviations were noticeable across all levels, a linear increment or decrement was observed in all quadrants. At the MP level, greater amounts of material, up to a maximum of 8 mm and 6 mm, were added to the posterolateral (Q1) and posteromedial (Q4) zones. In contrast, minimal material was added to the anterior zone. The rectifications in the lateral and medial regions were particularly significant, given their association with pressure-sensitive areas such as medial supracondylar (MSC) and lateral supracondylar (LSC) regions. This trend continued up to 10% of the cast length, with most of the material removal occurring at the anterior region of the cast. Material addition was observed at 25% of the cast length from 50° to 120°, indicating material incorporation in the fibular head areas. Corrections in prone-sensitive regions were evident with material removal up to 50° and beyond 120°, with a greater extent of removal seen posteriorly.

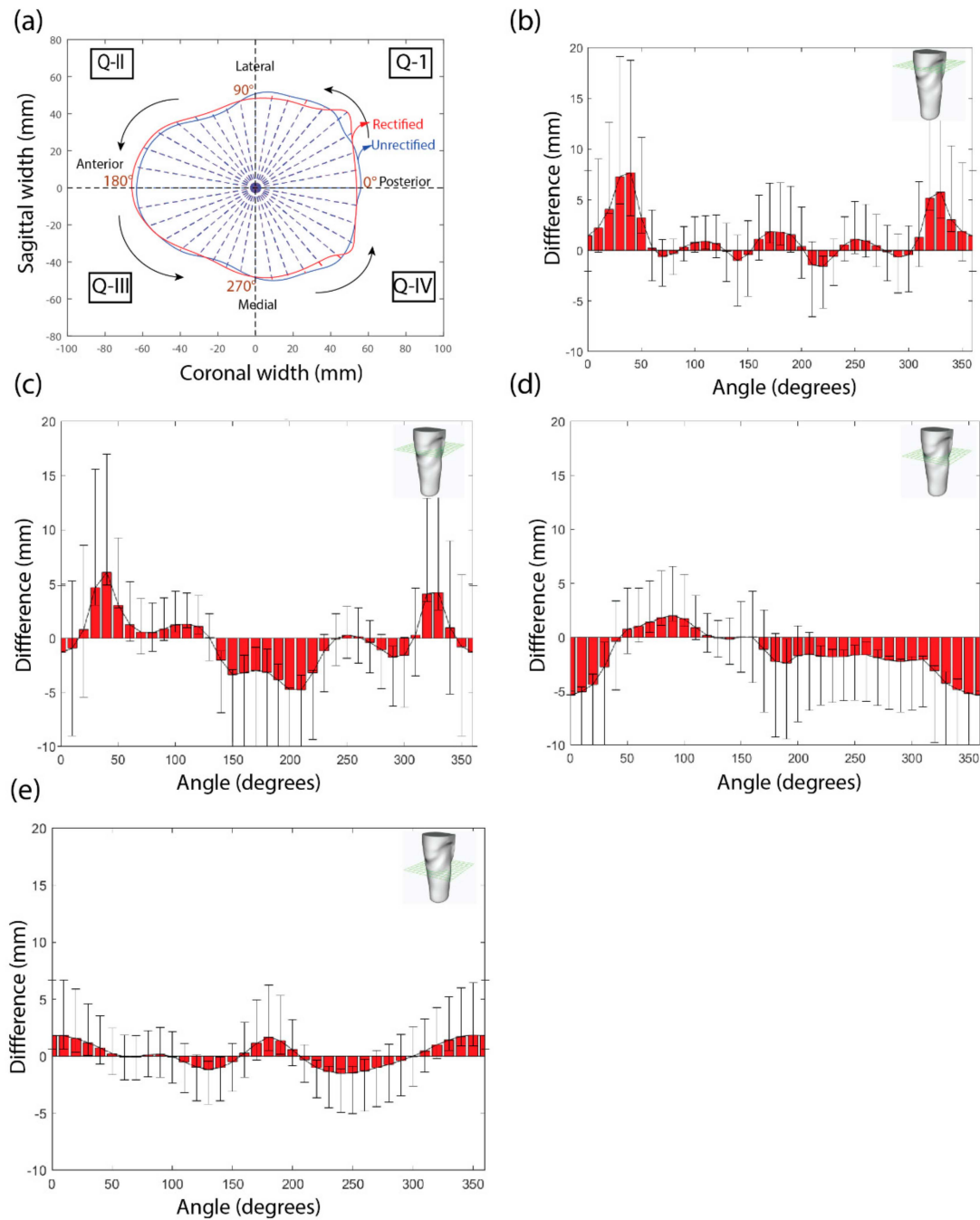


Figure 6. The measured absolute mean and standard error of the cross-sectional rectified cast: (a) The schematic representation of angular distance analysis for the entire circumference. (b) The measured angular change in the difference between RC and URC at mid-patella (b), as well as 10% (c), 25% (d) and 50% (e) of cast length.

The sagittal mean from Table 2 evidences that the material was trimmed off from the lateral and medial sides of the cast. Notably, at the lower part of the patella, the mean distance between the medial and lateral sides was notable, at -4.56 mm. The regions around 25% of the cast length encompass the socket’s sitting phase, underscoring the importance of rectification at this stage for ideal biomechanics and functionality.

Finally, at 50% of the cast length, where pressure-sensitive regions such as the lateral flare of the fibula and the tibia are prominent, the modification resulted in minimal material addition and removal around the stump. Specifically, the coronal width showed a mean difference of -0.82 mm, -0.79 mm, and -1.08 mm at 40%, 50%, and 60% of the cast length,

respectively, suggesting minimal material removal. In contrast, the sagittal width increased at the mid-stump level, with less material added to accommodate the flare of the fibula. These findings indicate that less correction was necessary at the mid-stump level.

In summary, the quantity of material added to load-sensitive regions, such as the medial flare of the calf (MFC) and lateral flare of the calf (LFC), was minimal. At the same time, a more substantial amount was removed from the medial flare of the thigh (MFT).

3.2. Categorisation of Casts

The preceding analysis of key locations offers insights into cast rectification with consideration for pressure-sensitive and tolerant areas. When comparing the difference between the rectified and unrectified perimeters along the cast's length, a linear trend in perimeter difference emerged for most amputees from 25% to 60% (Figure 7). However, beyond this point, deviations began to surface, with variations differing among individuals (see Figure 4a). Upon a closer examination of all amputee data, it became apparent that the deviation trend in the mid-stump region fell within the 60–90% range and varied among amputees.

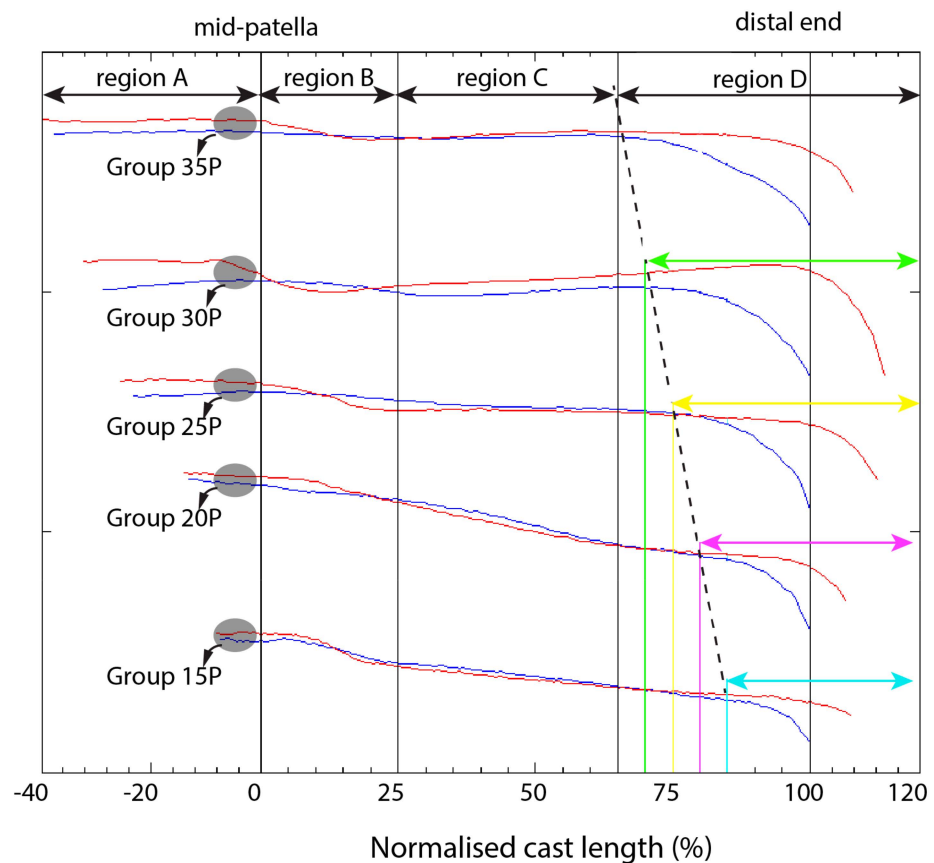


Figure 7. Classification of positive cast correction procedure as learned using the shape analysis tool (red curves show rectified and blue curves show unrectified sockets).

Consequently, the amputees were grouped based on these deviations to explore the correlations in the correction procedure. This evaluation led to the formation of five distinct groups, each corresponding to specific regions along the cast's length. The region above the mid-patella was labelled Region A, while the area from the patella to 25% of the cast's length became Region B. Region C commenced at 25% of the cast's length and concluded in alignment with each formed group. The five groups, derived from our observations, are described below.

Group 15P: In this category, linearity between the casts in Region C begins at 25% and terminates between 85 and 90% (equivalent to 15–10% of the length from the distal

end). The rectified plot follows a similar trend to that of unrectified casts after 25% and deviates between 10% and 15% from the distal end. Consequently, for this category, the limits of Region C are from 25% to 85% of the cast's length. Six amputees were classified into this category, where the linearity in Region C deviates between 85% and 90% of the cast's length. The area above 85% length is designated as Region D.

Group 20P: In this category, the trend in Region C starts at 25% and ends between 80 and 85% of the cast's length. The rectified plot closely follows the unrectified cast until 80% of the cast length. The area above 80% is considered as Region D.

Group 25P: Most amputees fit into this category, with the similarity in Region C deviating between 75% and 80% of the cast's length. This category has Region D encompassing the cast length above 75%.

Group 30P: In this category, the trend from Region C ends at between 70 and 75% of the cast's length. Region D includes the areas above 70% of the cast length.

Group 35P: Region C spans from 25% of the cast's length to 65%, with Region D comprising the areas above 65% of the cast length.

Patients' data were classified into these groups. Hypothesis analyses involving *t*-tests and *p*-tests were conducted on the data sets for statistical evaluation. Consequently, these tests aimed to determine whether observations were statistically significant, and assess the strength of the evidence suggesting that a result was not merely a chance occurrence. The null hypothesis (H_0) states that there was no relationship or difference between the two variables, while the alternative hypothesis asserts that the two sets of variables exhibited a significant disparity. The tests were applied to the difference between the rectified and unrectified perimeter data at various localities.

On comparing the datasets at 40% and 60% of the cast length, the *p*-value was found to be 0.40, with a *t*-test score of -0.82 (see Table 3). A smaller *p*-value and a higher *t*-score indicate greater similarity between the groups and stronger evidence favoring the alternative hypothesis. Comparing the datasets at the mid-stump level (40% and 60%) revealed more similarity between the datasets than between 60% and the lower limit of each group.

Table 3. Statistical analysis of the classified regions.

Dataset Comparison of Difference in Perimeter between	<i>p</i> -Value	<i>t</i> -Test
40% and 60% cast length	0.40	-0.82
60% and lower limit of group	0.30	-1.04
Lower limit and higher limit of group	0.17	1.35

For instance, Group 15P had a lower limit of 85% length and an upper limit of 90% length. Similarly, when analysing each group's lower and upper limits, the test results showed a low *p*-value (0.17) and a high *t*-test score (1.35). These results suggest that some deviation occurred between these limits, indicating less similarity between the datasets and the influence of non-random factors. Although a *p*-value less than 0.05 is typically considered statistically significant, a statistical analysis was conducted to assess the likelihood of the observed deviations in these classified groups.

3.3. Volume Comparison of Classified Regions

The assessment of volume differences between a patient's RC and URC considered both total volume variations and region-specific classifications. Figure 8a presents the total volume differences across all the studied subjects. Notably, regardless of URC volume, a consistent pattern emerges in the quantity of material added. The plot illustrates that many subjects cluster around a mean value of 13.1%. When the data are grouped, the

highest differences, 35.1% and 32.4%, fall within the 5–10% and 10–15% difference bands, respectively.

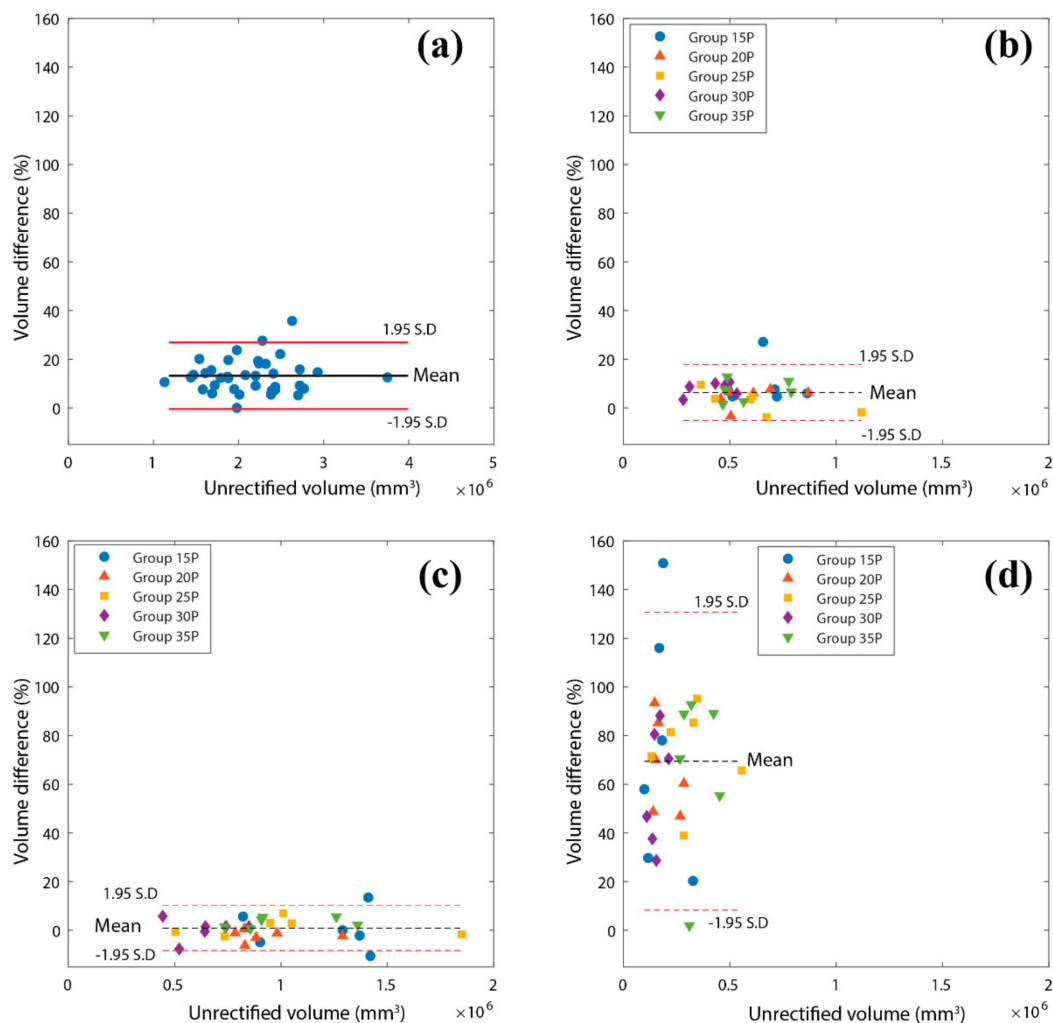


Figure 8. The generated volume difference between rectified and unrectified casts' (a) total volumes irrespective of groups; (b) Region B for different groups; (c) Region C for different groups; (d) Region D for different groups.

Now, considering the volume differences based on categorised regions (Figure 8b–d), the plot reveals that most rectification efforts were concentrated in Region D of the cast (Figure 8d). Rectification in the distal end primarily depends on the nature and shape of the stump, resulting in the highest mean difference of 69% within that region. Furthermore, 43.2% of subjects exhibited volume differences within the 60–90% range.

In contrast, Region B, encompassing more pressure-sensitive areas such as the patella, patella tendon, head of the tibia and fibula, displayed a mean difference of 6.0%, with a frequency distribution of 40.5% and 29.7% within the 5–10% and 0–5% difference bands, respectively. Finally, Region C exhibited minimal rectification, with a mean difference of 0.73%. Remarkably, 70.3% of amputees' casts showed differences within this region's −5% and 5% range of volume difference. This finding indicates consistently low rectification in this region, irrespective of the volume of the unrectified socket.

4. Discussion

This study was centered on exploring 3D surface scanning and assessing the trends and correlations in the shape, volume, and length of unrectified sockets compared to

expert-designed sockets. It assessed the viability of constructing data-driven models with the AmpScan tool and explored the ability to categorize patients based on the extent of rectification. This approach aims to train junior clinicians individually, moving away from reliance on a generalized population-based model. Surface analysis was employed to capture the overall shape of both rectified and unrectified sockets.

A principal factor that influences the comfort of the final socket is the presence of pressure-sensitive and tolerant areas. The evaluation of user, functional, and clinical preferences for TSB and PTB sockets is a challenging process. It greatly depends on the liners and accessories that are coupled with them. The study meticulously scrutinized the obtained results to identify correspondences and variances in the design and anatomy of rectified and unrectified sockets. These findings could serve as valuable training datasets for both ML models and clinicians. A further advantage of the generated datasets is their ability to enable direct socket rectification knowledge. Previous research utilized a reference shape library to scale and induce modifications, but this approach was proven to be ineffective and subsequently discontinued [34,35].

The statistical model employed in this study provided detailed insights into various shape profiles. Most notably, it revealed that most rectification occurred at the distal end of the socket, a phenomenon heavily dependent on the nature of the amputee's limb. However, when the distal end was excluded, the mid-patella region exhibited a substantial difference in perimeter, with a mean of 18 mm (4.8%).

Furthermore, a disparity in coronal and sagittal width differences along the length of the cast was established. Notably, the coronal width difference remained relatively constant up to 90% of the cast length, suggesting minimal rectification on the coronal side. Meanwhile, the sagittal plot displayed an increase along the length of the cast, indicating that most modifications occur on the sagittal side.

In summary, our comprehensive analysis highlights several key observations:

- At the patella, material was added to the anterior side and removed from the posterior side to create a flat end;
- Both the lateral and medial sides featured pressure-sensitive areas, resulting in material additions;
- At 25% length, the overall perimeter was reduced to accommodate pressure, with most material removal occurring in the sagittal plane;
- At the mid-stump level (40–60% length), minimal rectification was achieved by adding material to the sagittal plane.

The statistical plot revealed deviations at various intervals along the length of the cast (Table 3). The study identified five distinct groups with four specified regions, illustrating variations primarily in Region C and Region D of the sockets. It is essential to note that the extension of the rectified cast length depended on factors such as the maturity of the residual limb, its shape at the distal end, and the requirements of the prosthetic component based on amputation height, and the conical or cylindrical residual shape.

Limitations and Implications of the Study

While this study presents valuable insights, it has certain limitations. K-means clustering could be employed to conduct a more granular analysis of local rectification. The analysis revealed commonalities within the training population but did not offer a detailed socket design tailored to individual needs. Additionally, the study's applicability beyond the training population may be limited, as the model might struggle to provide relevant information for patients from diverse ethnic backgrounds or those with different causes of amputation, such as trauma, vascular disease, or road accidents.

Nonetheless, this study effectively demonstrated how to customise the socket design to fit general limb shapes. Regarding the training data, while more data would undoubtedly strengthen the study, the current dataset was considered adequate, encompassing a diverse range of individuals.

It is crucial to emphasise that the authors do not seek to fully automate the socket fabrication process, as this process remains deeply rooted in individual requirements. Instead, the aim is to empower junior clinicians with insights gained from past experiences, including data from expert prosthetists. This approach enables the generation of intelligent templates for socket design, streamlining the design process by allowing technicians to identify design trends in patients' residual limbs. Human input will be crucial throughout this process, ensuring that individual needs and specific designs are met. Thus, this study does not seek to replace the expertise of human clinicians, but rather to enhance their capabilities and efficiency in socket design.

5. Conclusions

This study successfully demonstrated a protocol for learning the intricacies of correction procedures and the general trends in residual limb cast shapes during prosthetic socket manufacturing, particularly in resource-constrained settings. With a commercial hand-held scanner, the efficacy in capturing the 3D geometry of both uncorrected and corrected positive casts of residual limbs was demonstrated. These digital geometries were subsequently subjected to automated shape analysis toolbox to quantify the extent of rectification performed on patients' residual limb casts.

Although this study was based on a limited dataset, it introduced a novel approach involving four distinct regions to assess the significance of correction procedures applied to the casts. The insights garnered from this analysis have the potential to benefit clinical researchers, offering an evidence-based tool for the evaluation of the performance of prosthetists-in-training. Moreover, it can offer foundational data for identifying the regions requiring rectification and assessing socket comfort during long-term follow-ups with individual patients. By streamlining this process, our method can reduce the clinical and iteration time necessary for crafting well-fitting, comfortable sockets.

Nonetheless, it is essential to acknowledge the study's limitations and exercise caution in its interpretation and application. The study encompasses only 50 patients from a specific ethnic background, thus limiting its generalizability to all patient populations and clinical scenarios. Moreover, it is crucial to emphasise that the manufacturing process should not be fully automated, as patients must remain involved as a paramount consideration in socket design and fabrication. Therefore, while our method offers valuable insights and efficiencies, it should be regarded as a complementary tool for the prosthetic socket manufacturing process, augmenting the expertise of clinicians rather than replacing it.

Author Contributions: Conceptualization, Y.R.N., K.K. and A.K.S.; formal analysis, Y.R.N.; funding acquisition, K.K.; methodology, Y.R.N. and K.K.; project administration, K.K. and P.M.; resources, A.K.S. and P.M.; software, Y.R.N.; supervision, F.F. and K.K.; visualization, F.F. and V.V.S.; writing—original draft, Y.R.N.; writing—review and editing, F.F. and V.V.S. All authors have read and agreed to the published version of the manuscript.

Funding: This research was funded by the Academy of Medical Sciences under Global Challenges Research Fund (GCRF) Scheme (grant number: GCRFNG\100125). The UK's Royal Academy of Engineering also financially supported this research work for the project "Upcycled Plastic Prosthetics" (grant reference: FF\1920\1\30).

Institutional Review Board Statement: Not applicable.

Informed Consent Statement: Not applicable.

Data Availability Statement: The data presented in this study are available on request from the corresponding author.

Acknowledgments: The authors gratefully thank the prosthetists from Bhagwan Mahaveer Viklang Sahayata Samiti (BMVSS) Jaipur, India, for their time and coordination in providing casts for scanning.

Conflicts of Interest: The authors declare no conflicts of interest.

References

1. Gailey, R.; Allen, K.; Castles, J.; Kucharick, J.; Roeder, M. Review of secondary physical conditions associated with lower-limb. *J. Rehabil. Res. Dev.* **2008**, *45*, 15–30. [[CrossRef](#)]
2. Dillingham, T.R.; Pezzin, L.E.; MacKenzie, E.J.; Burgess, A.R. Use and satisfaction with prosthetic devices among persons with trauma-related amputations: A long-term outcome study. *Am. J. Phys. Med. Rehabil.* **2001**, *80*, 563–571. [[CrossRef](#)] [[PubMed](#)]
3. Meulenbelt, H.E.; Geertzen, J.H.; Jonkman, M.F.; Dijkstra, P.U. Skin problems of the stump in lower limb amputees: 1. A clinical study. *Acta Derm. Venereol.* **2011**, *91*, 173–177. [[CrossRef](#)] [[PubMed](#)]
4. Nagarajan, Y.R.; Farukh, F.; Silberschmidt, V.V.; Kandan, K.; Rathore, R.; Singh, A.K.; Mukul, P. Strength Assessment of PET Composite Prosthetic Sockets. *Materials* **2023**, *16*, 4606. [[CrossRef](#)] [[PubMed](#)]
5. Stevens, P.M.; DePalma, R.R.; Wurdeman, S.R. Transtibial socket design, interface, and suspension: A clinical practice guideline. *JPO J. Prosthet. Orthot.* **2019**, *31*, 172–178. [[CrossRef](#)]
6. Foort, J. The patellar-tendon-bearing prosthesis for below-knee amputees, a review of technique and criteria. *Artif. Limbs* **1965**, *9*, 4–13.
7. Faustini, M.C.; Neptune, R.R.; Crawford, R.H.; Rogers, W.E.; Bosker, G. An experimental and theoretical framework for manufacturing prosthetic sockets for transtibial amputees. *IEEE Trans. Neural Syst. Rehabil. Eng.* **2006**, *14*, 304–310. [[CrossRef](#)]
8. Pezzin, L.E.; Dillingham, T.R.; MacKenzie, E.J.; Ephraim, P.; Rossbach, P. Use and satisfaction with prosthetic limb devices and related services. *Arch. Phys. Med. Rehabil.* **2004**, *85*, 723–729. [[CrossRef](#)]
9. Haggstrom, E.E.; Hansson, E.; Hagberg, K. Comparison of prosthetic costs and service between osseointegrated and conventional suspended transfemoral prostheses. *Prosthet. Orthot. Int.* **2013**, *37*, 152–160. [[CrossRef](#)]
10. Convery, P.; Buis, A.; Wilkie, R.; Sockalingam, S.; Blair, A.; McHugh, B. Measurement of the consistency of patellar-tendon-bearing cast rectification. *Prosthet. Orthot. Int.* **2003**, *27*, 207–213. [[CrossRef](#)] [[PubMed](#)]
11. Dickinson, A.S.; Steer, J.W.; Woods, C.J.; Worsley, P.R. Registering a methodology for imaging and analysis of residual-limb shape after transtibial amputation. *J. Rehabil. Res. Dev.* **2016**, *53*, 207–218. [[CrossRef](#)] [[PubMed](#)]
12. Yiğiter, K.; Şener, G.; Bayar, K. Comparison of the effects of patellar tendon bearing and total surface bearing sockets on prosthetic fitting and rehabilitation. *Prosthet. Orthot. Int.* **2002**, *26*, 206–212. [[CrossRef](#)] [[PubMed](#)]
13. Hachisuka, K.; Dozono, K.; Ogata, H.; Ohmine, S.; Shitama, H.; Shinkoda, K. Total surface bearing below-knee prosthesis: Advantages, disadvantages, and clinical implications. *Arch. Phys. Med. Rehabil.* **1998**, *79*, 783–789. [[CrossRef](#)]
14. Ryniewicz, W.I.; Ryniewicz, A.M.; Wiśniewska, G. The evaluation of the accuracy of shape imaging of prosthetic abutment. *Acta Bioeng. Biomech.* **2016**, *18*, 43–50. [[PubMed](#)]
15. Laing, S.; Lythgo, N.; Lavranos, J.; Lee, P.V.S. Transtibial prosthetic socket shape in a developing country: A study to compare initial outcomes in pressure cast hydrostatic and patella tendon bearing designs. *Gait Posture* **2017**, *58*, 363–368. [[CrossRef](#)]
16. Sanders, J.E.; Fatone, S. Residual limb volume change: Systematic review of measurement and management. *J. Rehabil. Res. Dev.* **2011**, *48*, 949. [[CrossRef](#)]
17. Ozen, M.; Sayman, O.; Havitcioglu, H. Modeling and stress analyses of a normal foot-ankle and a prosthetic foot-ankle complex. *Acta Bioeng. Biomech.* **2013**, *15*, 19–27.
18. Suresh, N.; Janakiram, C.; Nayar, S.; Krishnapriya, V.N.; Mathew, A. Effectiveness of digital data acquisition technologies in the fabrication of maxillofacial prostheses—A systematic review. *J. Oral Biol. Craniofacial Res.* **2022**, *12*, 208–215. [[CrossRef](#)]
19. Colombo, G.; Filippi, S.; Rizzi, C.; Rotini, F. A new design paradigm for the development of custom-fit soft sockets for lower limb prostheses. *Comput. Ind.* **2010**, *61*, 513–523. [[CrossRef](#)]
20. Buzzi, M.; Colombo, G.; Facoetti, G.; Gabbiadini, S.; Rizzi, C. 3D modelling and knowledge: Tools to automate prosthesis development process. *Int. J. Interact. Des. Manuf.* **2012**, *6*, 41–53. [[CrossRef](#)]
21. Cabrera, I.A.; Pike, T.C.; McKittrick, J.M.; Meyers, M.A.; Rao, R.R.; Lin, A.Y. Digital healthcare technologies: Modern tools to transform prosthetic care. *Expert Rev. Med. Devices* **2021**, *18*, 129–144. [[CrossRef](#)]
22. Seminati, E.; Canepa Talamas, D.; Young, M.; Twiste, M.; Dhokia, V.; Bilzon, J.L. Validity and reliability of a novel 3D scanner for assessment of the shape and volume of amputees' residual limb models. *PLoS ONE* **2017**, *12*, e0184498. [[CrossRef](#)]
23. Steer, J.W.; Grudniewski, P.A.; Browne, M.; Worsley, P.R.; Sobey, A.J.; Dickinson, A.S. Predictive prosthetic socket design: Part 2—Generating person-specific candidate designs using multi-objective genetic algorithms. *Biomech. Model. Mechanobiol.* **2020**, *19*, 1347–1360. [[CrossRef](#)] [[PubMed](#)]
24. Li, S.; Lan, H.; Luo, X.; Lv, Y.; Gao, L.; Yu, H. Quantitative compensation design for prosthetic socket based on eigenvector algorithm method. *Rev. Sci. Instrum.* **2019**, *90*, 104101. [[CrossRef](#)]
25. Ballit, A.; Mougharbel, I.; Ghaziri, H.; Dao, T. Computer-aided parametric prosthetic socket design based on real-time soft tissue deformation and an inverse approach. *Vis. Comput.* **2022**, *38*, 919–937. [[CrossRef](#)]
26. Sewell, P.; Noroozi, S.; Vinney, J.; Amali, R.; Andrews, S. Static and dynamic pressure prediction for prosthetic socket fitting assessment utilising an inverse problem approach. *Artif. Intell. Med.* **2012**, *54*, 29–41. [[CrossRef](#)] [[PubMed](#)]
27. Karamousadakis, M.; Porichis, A.; Ottikkutti, S.; Chen, D.; Vartholomeos, P. A sensor-based decision support system for transfemoral socket rectification. *Sensors* **2021**, *21*, 3743. [[CrossRef](#)] [[PubMed](#)]
28. Steer, J.; Stocks, O.; Parsons, J.; Worsley, P.; Dickinson, A. Ampscan: A lightweight Python package for shape analysis of prosthetics and orthotics. *J. Open Source Softw.* **2020**, *5*, 2060. [[CrossRef](#)]

29. Zheng, Y.; Mak, A.F.; Leung, A.K. State-of-the-art methods for geometric and biomechanical assessments of residual limbs: A review. *J. Rehabil. Res. Dev.* **2001**, *38*, 487–504.
30. Bolt, A.; de Boer-Wilzing, V.G.; Geertzen, J.; Emmelot, C.H.; Baars, E.; Dijkstra, P.U. Variation in measurements of transtibial stump model volume: A comparison of five methods. *Am. J. Phys. Med. Rehabil.* **2010**, *89*, 376–384. [[CrossRef](#)]
31. Mehmood, W.; Abd Razak, N.A.; Lau, M.S.; Chung, T.Y.; Gholizadeh, H.; Abu Osman, N.A. Comparative study of the circumferential and volumetric analysis between conventional casting and three-dimensional scanning methods for transtibial socket: A preliminary study. *Proc. Inst. Mech. Eng. Part H J. Eng. Med.* **2019**, *233*, 181–192. [[CrossRef](#)] [[PubMed](#)]
32. Ryniewicz, A.M.; Ryniewicz, W.I. Microstructural and micromechanical tests of titanium biomaterials intended for prosthetic reconstructions. *Acta Bioeng. Biomech.* **2016**, *18*, 121–127. [[PubMed](#)]
33. Won, N.Y.; Paul, A.; Garibaldi, M.; Baumgartner, R.E.; Kaufman, K.R.; Reider, L.; Wrigley, J.; Morshed, S. Scoping review to evaluate existing measurement parameters and clinical outcomes of transtibial prosthetic alignment and socket fit. *Prosthet. Orthot. Int.* **2022**, *46*, 95–107. [[CrossRef](#)] [[PubMed](#)]
34. Engsborg, J.R.; Clynch, G.S.; Lee, A.G.; Allan, J.S.; Harder, J.A. A CAD CAM method for custom below-knee sockets. *Prosthet. Orthot. Int.* **1992**, *16*, 183–188. [[CrossRef](#)]
35. Torres-Moreno, R.; Foort, J.; Morrison, J.B.; Saunders, C.G. A reference shape library for computer aided socket design in above-knee prostheses. *Prosthet. Orthot. Int.* **1989**, *13*, 130–139. [[CrossRef](#)]

Disclaimer/Publisher’s Note: The statements, opinions and data contained in all publications are solely those of the individual author(s) and contributor(s) and not of MDPI and/or the editor(s). MDPI and/or the editor(s) disclaim responsibility for any injury to people or property resulting from any ideas, methods, instructions or products referred to in the content.